ATOMIC PHYSICS AND ECR SOURCE

M. Cavenago

I.N.F.N Laboratori Nazionali di Legnaro

ATOMIC PHYSICS AND THE ECR ION SOURCE

Marco Cavenago

Laboratori Nazionali di Legnaro, via Romea n. 4 , I-35020 Legnaro (PD) Italy

O K

2-7-91

ATOMIC PHYSICS AND THE ECR ION SOURCE *

Marco Cavenago

Laboratori Nazionali di Legnaro, via Romea n. 4 , I-35020 Legnaro (PD) Italy

After reviewing the Electron Cyclotron Resonance Ion Source in construction at Legnaro, a survey of some atomic physics topics, spanning from QED precision tests to ion-atom collisions at several energies is given. The importance of ion-atom and ion-ion cross section to the physics of the ECRIS itself is emphasized. Few experiments suitable the Legnaro installation are briefly discussed. A case is proposed for the boron-boron charge exchange cross section, of interest in beam trapping and aneutronic fusion concepts. Exact results for trapping into a two mirror magnetic bottle and an adiabatic invariant in the case of an ECR ion source are given.

I) INTRODUCTION

While the simple hydrogen atom is well-known as the exemplar case of quantum mechanics to all physicists, the other atoms are the object of few specialists: since the nucleus charge Ze and the electron cloud charge are equal, the attraction felt by the outermost electrons is strongly dependent on the details of the electron configuration, as seen in the periodic table. The availability (table I) of highly stripped ions lead us to different regimes, where different and somewhat simpler regularity appears.

In a first instance, the hydrogen-like and helium-like ions [1] represent a natural laboratory to study radiative QED corrections to the electron energy levels, going as $\alpha(Z\alpha)^4$, while the perturbing interaction energy between the electrons goes as $\alpha(Z\alpha)$.

It should anyway be appreciated that the transition energies [2,3] are $\hbar\omega \propto (Z\alpha)^2$ and this makes spectroscopy more difficult; in particular [4] , the natural line width is $\Gamma \propto (\hbar\omega)^3 d^2$, where d is the dipole transition matrix element. For a given line, $d \propto 1/Z\alpha$ and then $\Gamma \propto (Z\alpha)^4$.

Other interesting phenomena, more pertinent to the ions usually extracted from an Electron Cyclotron Resonance Ion Source [5], stem out from the potential energy which is stored in a highly charged ion A^{z+}, sufficient to produce the transfer ionization of other atoms B :

$$A^{z+} + B \rightarrow A^{(u-m)+ *} + B^{(z+m-u)+} \rightarrow A^{u+} + B^{(z+m-u)+} + m\,e \qquad ,(1)$$
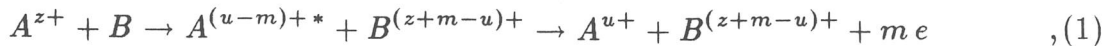
where m electrons are expelled in the relaxation of the excited atom A^* ; here $m \geq 0$; the case of a initially ionized B will also be considered in this paper (see Eq. (5) later).

The initial ion charge z of course decreases to u, and the captured electrons may jump into the ground state A^{u+} or into the metastable states $A^{u+\,'}$, that are states not strongly coupled by optical or dielectronic transitions to the ground state A^{u+} , and therefore are states of difficult excitation from the ground state. The possibility of preparing the

---

metastable states $A^{u+\prime}$ from a higher charged state and selecting them [6,7] is thus most valuable (table I).

Similarly, the potential energy stored in a highly charged ion makes other particular applications possible, such as X-ray lasers [8] with small efficiency, or ion polarization through capture of a polarized electron from a beam of polarized Na^+ [9].

Electrons are captured by A at large (order of $10\mathring{A}$) distances, depending on its high charge (see Eq. (10)) . The cross sections may be as high as $10^{-14} cm^2$ for a relative ion velocity of the order of $1 \ a.u. = \alpha c$, corresponding to the energy $E/A = 24 keV/u$, and similar values for smaller relative velocity corresponding to $E/A \cong 10 eV/u$ typical of an ECRIS plasma.

In the latter case transfer ionization is evidently one limiting factor of the source performance [10],[11] , the other being the ion confinement time. Studying the reactions of the extracted ions from an ECR source we improve the understanding of what is going on in the source and in similar plasmas. We therefore will focus on transfer ionization in section III to V of this paper.

We can also define a high velocity regime (see table I) in the collision of the ion A against B (a target atom or another ion) by requiring that the B electrons have sufficient energy (in the frame of A) to probe the L or M shells of the ion A ; since typically few keV of kinetic energy are needed, the high velocity regime requires $E/A \gg 1 MeV/u$ ion beams, usually provided by nuclear physics facilities. Collision may result in further ionization of A (stripping) or capture of electron in the above mentioned shells of A.

In magnetically confined thermonuclear plasmas [12], the relevance of atomic physics of several ions is mainly related to the unavoidable presence of iron impurities from the vessel walls [13] . In the context of inertial confinement fusion [14], (abbreviation ICF), the necessarily liquid FLiBe walls provide an abundant vapor of B atoms which may affect the ion beam A propagation, designed to hit the fusion pellet: the electrons from the ionization of B partly neutralize the beam A , which fact is beneficial for the beam focusing, but may lead to beam instability [15]. Moreover A may be further ionizated by the photon flux from the progressivily heating pellet.

The well known non-Liouvillian stacking concept [16] may exploit several atomic physics processes, as the photoionization of A^+ or the stimulated recombination $A^{++} + e + h\nu \rightarrow A^+ + 2h\nu$; see Ref. [17, 18] . The wider subject of ion beam manipulation by means of atomic physics reactions reaction includes the well known laser cooling or the proposed intrabeam collision cooling [19] .

The electrodynamics interaction [20] of fast heavy ion approaching each other within a few $10^{-12} cm$ features also strong perturbation of the vacuum with expected positron creation [21], emission of very hard Auger electron (100 keV) [22] and, for GeV/u ion energies, emission of pions and, maybe, other still unknown particles [23]. These more fascinating topics are outside the scope of the present paper.

II) ALICE

In the ECR concept [11], a low pressure gas $p \cong 10^{-7} torr$ is ionized and heated by a microwave radiation, where the magnetic field satisfies the cyclotron resonance condition

for electrons [24] :

$$|\vec{B}(\vec{x})| = B_{ecr} = \frac{mc\omega}{e} \qquad (2)$$

The present trends in ECR design favour a high magnetic field at the walls, B_{max} , which reflects a longer ion confinement time $\tau \cong 10^{-2}s$ and, less directly, a high frequency ω which permits to store and heat a denser plasma $\omega^2 \gg \omega_{pl}^2 = 4\pi e^2 n_e/m$. For this reason, the ratio B_{max}/B_{ecr} is as high as two in some recent design; in our it is 1.44 .

The ECR ion source in construction at Legnaro, named Alice, is a small 14.4 Ghz multipurpose source (see Fig. 1), whose magnetic field configuration was careful optimized for reduced power consumption [25] and where the plasma chamber may be easily removed and substituted, with the purpose of switching from one metallic ion to another.

Apart from this cooled removable plasma chamber, its design and dimension does not differ significantly from some successful 14.5 Ghz sources, recently come into operation [26], such as Caprice or ECR4 , which gave satisfying results as well as the 14.5 Ghz Advanced ECR at Berkeley did. The latter source is considerably larger than the previous two, and can therefore easily house an electron gun, apparently beneficial for the source performance and the plasma stability.

The typical yield for the most abundant charge state is $10^{-4}A$ and electrical currents of $1\mu A$ for a charge state as high as 32+ for uranium or 15+ for argon may be extracted; nanoamperes of 17+ and bare argon are sometimes available.

The access to the source Alice for further equipment was a constant care in the design, due to its limited dimension, and is possible through the so-called expansion port, a slanted CF100 flange (see Fig. 2), or by changing the removable plasma chamber: in particular an electron gun might be easily mounted.

The relevant atomic processes in an ECRIS source are: i) the impact ionization ii) the impact Auger multiionization iii) the transfer ionization (and their inverse reactions). The impact ionization is:

$$A^{z+} + e \rightarrow A^{(z+1)+} + 2e \qquad (3)$$

where the inverse reaction is depressed by the fact that the right hand side electrons are promptly accelerated by the microwave field. For $z = 32$ and the uranium ion case, the ionization energy is $I = 2.5 \ keV$; the maximum cross section is of the order $10^{-18} \div 10^{-17}cm^{-2}$ for an electron energy $E \cong 5I$.

Since we know from bremsstrahlung spectra that high energy electrons $E \cong 100keV$ are present in the ECR plasma, we conclude that they are too energetic to be effectively dragged by reaction (3) and there must also be ii) K-shell ionization or Auger multiionization

$$A^{z+} + e \rightarrow A^{(z+1)+ *} + 2e \rightarrow A^{(z+s)} + (s+1)e \qquad (4)$$
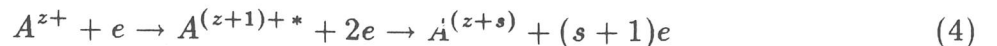
Indeed even the spectral lines K_α and K_β may be observed from a source [27], even if the corresponding hydrogen-like ion cannot be extracted. Similar experiments are easily done with an Electron Beam Ion Trap [28,29] .

The ions are heated from electron collisions up to a negligible extent (10 eV) and their velocity is $10^{-4} \div 10^{-3}$ times the electron speed; but the cross section σ of the transfer ionization (1) are very large ($10^{-14}cm^2$) since the energy is supplied by A itself; as we

anticipated from Eq. (10) , they correspond to an impact parameter of 20 Bohr radii. So the rates $\cong n_A n_B < v_{rel}\sigma >$ of this reaction may be considerably high and this process limits the highest available charge state; here $v_{rel} = |v_A - v_B|$. Reaction (1) is luckily depressed by the limited amount of neutral gas available inside an ECR plasma.

This motivates us to consider also the more general transfer reaction

$$A^{z+} + B^{t+} \rightarrow A^{(z-s+t)+\,*} + B^{s+} \rightarrow A^{u+} + B^{s+} + (u + s - t - r)\,e \qquad (5)$$
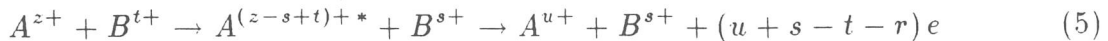
where B is a lower charge state ion. In turn reaction (5) is depressed by Coulomb repulsion, when $\beta \ll \alpha$ as it is in ECR ion sources, and is therefore strongly energy dependent (see later Eq. (16)).

A particular case of (1) is the resonant electron exchange, for example when $A = B$ and $z = t + 1 = u + 1 = s$.

The difficult modelling of an ECR plasma is also due to the limited data available on process (3) through (5) , which are usually accounted for by the effective rates [10],[30] . Of course, it is evident that basic requirements such as the need of exposing the ion A^{z+} to enough electron bombardment and a low neutral pressure are important. The electron bombardment is measured by

$$n_e\,\tau_i(z) \, < v_e \sigma_{ion} > \, \geq 1 \qquad (6)$$

where σ_{ion} is mostly contributed by Eq. (3) and the average is taken on the electron velocity distribution; here the ion confinement time $\tau_i(z)$ depends on its own charge.

The low neutral pressure is evidently helpful, since it reduces the rates of the reactions (1) and (5) ; note that Eqs. (1) , (3) and (4) provide an ionic pumping.

We speculate that the important experimental phenomena of gas mixing [31] may also be related to (1) and (5) : the lighter ions are easily fully ionized, they can not spoil the desired high charge state heavy ion A^{z+} and they can reduce the collisions of A^{z+} with the neutral gas B , by cooling A^{z+} or ionizing B . Transport phenomena due to atomic collisions and transfer ionization should be potentially important in an ECRIS, if they are still sensible at the small level of impurities (all nuclei with $A > 4$) of conventional fusion plasmas[13] .

III) TRANSFER IONIZATION MODELS

In the transfer reaction (1) we can measure the final state only, but several information are available. It is worthwhile to remember some basic experimental methods.

First of all, in the medium energy regime, the ion beam emerges nearly straight from the reaction with some kinetic energy gain, of the order of $10\,eV$; the incident ion A^{z+} energy may be defined as well as $0.16z\,eV$ FWHM by filtering the beam from an appropriate source with a deceleration , a hemispherical electrostatic analyzer, and an acceleration [32] ; the ion final energy may be measured with similar devices and precision. This measurement of the energy gain of A is called transactional spectroscopy. Its validity ceases for high energy ions.

The electrons (say at $500\,eV$) are emitted on the whole solid angle, and the precision detectors, based on electrostatic deceleration, may collect only a small part of them. Therefore the high current of ECR ion sources is very helpful for electron spectroscopy.

The existence of the intermediate state of Eq. (1) is inferred by observing distinct peaks in the kinetic energy gain of the ion A^{u+}, interpreted as several values of m. Note that the potential energy liberated by A in the first step (also named charge exchange rection) is converted into kinetic energy of the ions, while the energy liberated in the second step is given to the electrons.

Electron emission is impossible in the case of one electron exchange $u = z - 1$ which implies $m = 0$. Photon may be always emitted by A^*, and can be detected with grazing incidence gratings in the range $O(10)\,eV < \hbar\omega < O(1000)eV$ (above this energy crystal spectrometers are used).

The transfer of one electron is well described by the classical overbarrier model [33,34], when the relative ion velocity β is much less than the orbital velocity of the active electron: $\beta < \alpha$. When the electron is bound to B, its energy is $-I$ plus the perturbation of the field of A, that is $-ze^2/R$ where R is the slowly changing internuclear separation (we will see that R is much greater than the Bohr radius). If the electron jumped to A into the high level n, the electron energy would become $-mz^2e^4/2n^2\hbar^2$ as given by the Bohr formula approximately valid for Rydberg atoms, plus the perturbation $-e^2/R$ of the then charged B; due to the adiabaticity of the ion motion, the electron total energy E_e would be conserved:

$$E_e = -I - \frac{ze^2}{R} = -\frac{mz^2e^4}{2n^2\hbar^2} - \frac{e^2}{R} \tag{7}$$

The model assumes that the transfer actually takes place only if the electron can pass the barrier due to its potential energy V in the field of the ions A^{z+} and B^+. The minimum barrier to pass is the saddle point of V, which is determined as the maximum point of V on the line AB: since $V(x) = -e^2(x^{-1} + z(R-x)^{-1})$ where x is the electron distance from B, this barrier is $-e^2(z^{1/2} + 1)^2/R$. Therefore if

$$E_e > -\frac{e^2(z^{1/2} + 1)^2}{R} \tag{8}$$

the transfer takes place with a probability near one because of Eq. (7), which is also a resonance condition.

According to Eqs. (7) and (8) the capture into the n-th orbital is possible if $n < N$ where N is the integer part of

$$z\sqrt{\frac{me^4}{2\hbar^2 I}\frac{2z^{1/2} + 1}{z + 2z^{1/2}}} \tag{9}$$

and it happens for $R < R_n$ with:

$$R_n = \frac{2\hbar^2}{me^2}\frac{z - 1}{(z^2/n^2) - (I/13.6eV)} < R_N \cong \frac{e^2}{I}(2z^{1/2} + 1) \tag{10}$$

The model assumes that the total cross section is related to the larger capture radius $\sigma\pi R_N^2$ and that the contribution of each orbital n is $\pi(R_n^2 - R_{n-1}^2)$.

5

The energy gain Q of the ion A can also be determined: since the electron is transferred when $R = R_N$, the repulsion between the two newly formed ions provides the energy $e^2(z-1)/R_N$ to A plus B and

$$Q \cong \frac{M_B}{M_A + M_B} \frac{e^2(r-1)}{R_N} \geq I \frac{M_B}{M_A + M_B} \left(\frac{z-1}{2z^{1/2}+1} \right) \qquad (11)$$

Two extensions are natural; the case of ion-ion collisions (5) , with the cross section depressed by the repulsion between the approaching ions, (still a considerable section if $z \gg t$), and the case of multiple electron transfer.

Indeed let us consider the transfer of $k = s - t$ electrons in (5) . Let $I_B[s - k \to s]$ be the binding energy of these k electron to B and $I_A^*[z - k \to z]$ the binding to A in the excited intermediate state; including the perturbation of the other ion, the total energy $E_e(k)$ balance of these electrons is:

$$E_e(k) = -I_B[s - k \to s] - \frac{z\,k\,e^2}{R} = -I_A^*[z - k \to z] - \frac{s\,k\,e^2}{R} \qquad (12)$$

from which the reaction distance R_c is promptly related to the final state:

$$R_c = \frac{e^2 k(z - s)}{I_A^*[z - k \to z] - I_B[s - k \to s]} \qquad (13)$$

In the case of one electron transfer, the classical overbarrier gives the condition [2,35]:

$$E_e(1) > -\frac{e^2(z^{1/2} + s^{1/2})^2}{R} \qquad (14)$$

which determines the final state binding energy I_A^* and therefore the capture radius R_c :

$$R_c \cong \frac{e^2}{I(s)} (2\sqrt{zs} + s) \qquad\qquad ; (15)$$

evidently the s-th ionization potential of B, written as $I(s) \equiv I_B[s - 1 \to s]$ for brevity, is strongly increasing with s .

Let b be the larger impact parameter which allows the ions A^{z+} and $B^{(s-1)+}$ to come closer than the one electron capture radius R_c ; then $\sigma = \pi b^2$ is the expected inclusive cross section for ion-ion charge exchange of at least one electron. From simple kinematics we find

$$\sigma = \pi R_c^2 \left(1 - \frac{I(s)}{E_{cm}} \frac{z(s-1)}{s + 2\sqrt{z\,s}} \right) \qquad (16)$$

where $E_{cm} = \frac{1}{2}(\vec{v}_A - \vec{v}_B)^2 M_A M_B / M_A + M_B$ is the collision energy; the above formula is meaningful when $\sigma \geq 0$, which requires a collision energy $E_{cm} \geq I(s)z(s-1)/s + 2(zs)^{1/2}$.

In particular the bare argon should fear the Ar^+ collision ($z = 18, s = 2$) only when $E_{cm} > (18/14)I(s)$; it is unclear whether this condition is satisfied in the ECR ion source

6

plasma. Moreover the ion-ion transfer ionization itself heats the plasma ions. On the other side, this condition is surely satisfied when the ion temperature is high (10 keV).

In the case of multiple electron transfer $k > 1$ several generalizations of Eq. (14) are possible : the electrons may be transferred together or in a sequence [36] .

IV) BEAM INJECTION INTO ECR ION SOURCES

The injection of a boron B^+ ion beam (or possibly a B^{++} beam) into an ECR ion source, while the source itself, fed by borane $(n(BH_3))$, is producing a plasma which contains cold boron ions, cold protons and hot electrons may offer relevant informations on the source status and the interesting subject of beam-plasma fusion (see Fig. 3).

The beam-plasma concepts [37,38] and the Migma concept [39] exploit the fact that the ion beam is not affected by friction from the electrons when their temperature T_e is very high as it is in a ECR ion source:

$$\frac{dE}{dx} = -\frac{2\pi z e^4 \ln \Lambda}{E} \left(\frac{4n_e}{3\sqrt{\pi}} \left(\frac{m_e}{M_A} \right)^{1/2} \left(\frac{E}{T_e} \right)^{3/2} + M_A \sum_i \frac{n_i z_i}{M_i} \right) \qquad (17)$$

where $\ln \Lambda$ is about 20 and n_i , z_i and M_i are respectively the density, the charge state and the mass of the i-th ion species in the plasma.

A considerable number of fusion reactions and eventually more energy than the beam energy itself may be produced; the case of neutral atom beam injection, or better, neutral plasma injection is well known [37] .

A distinctive feature of the present concept is the use of charged beam, easily manageable also in small scale experiments; trapping of the beam is then the relevant open question. A f fraction of the injected beam is kicked out of its initial trajectory by the charge exchange reaction

$$B^+(beam) + B^{++}(plasma) \rightarrow B^{++}(beam) + B^+(plasma) \qquad (18)$$
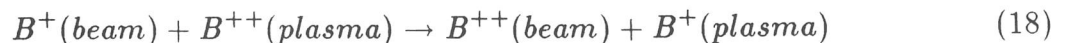
and the similar reactions (1) ,(3) and (5) , while the fraction $1 - f$ keeps following Hamiltonian mechanics. Different and less available fuels (^{3}He) may be also considered.

It is well known that the latter fraction will exit from the plasma after travelling a path length L ; common lore blames the Liouville theorem for it. A simple and explicit verification is available in mirror-like systems (see appendix A) that, even if not integrable, still have two invariants of motion, the energy and canonical angular momentum, thanks to which we show that the beam will return where it was injected, if it is not lost before.

The fraction f may be estimated as $n_B \sigma L_p$ where the cross section σ of reaction (18) may be estimated by Eq. (16) and measured with the experiments ii) of section V, and the length of the beam path in the plasma L_p is easily determined for each given machine. Since $n_B < 10^{12} cm^{-3}$ and $\sigma < 10^{-14} cm^{-2}$ even with optimistic estimates, we find that $L_p > 100 cm$ is necessary in order to trap a significant fraction.

If we think of a practical size machine, L_p may well be few meters, and moreover the fraction $1 - f$ of the beam may be circulated again; so that a small f , the fraction of the scattered beam, is not a limit to this scheme.

The fraction f splits into two fractions, the fraction wf of ions whose angular momentum changes in a way to prevent the beam return to the walls, and the fraction $f(1-w)$ whose momentum change is not enough to prevent the ejection of beam or is enhancing the ejection. The capture process is due to the fact that the ion gyroradius halfens when a B^+ ion becomes a B^{++} ion.

The case of ion injected at the midplane of a simple mirror system was previously studied in the context of the Migma concept [39]. We show in appendix A that w may be different from zero even in the less intuitive case of beam injection from outside the mirror region.

From data [40] of the nuclear reaction cross section

$$p +^{11}B \rightarrow 3 {}^{4}\text{He} \tag{19}$$

we see that we reach a more or less constant cross section of $0.5 \ 10^{-24} cm^{-2}$ for a $0.4 MeV/u$ boron beam. From Fig. 3 we see that, in order to bend the beam, we need:

$$r_w B_m > r B_z = \frac{c}{ze}\sqrt{2M_A E} \tag{20}$$

where the minimum magnetic field is $B_m \cong (9/10)B_{ecr}$ in the middle of the two mirror, and r_w is the radius of the vacuum vessel. The length L of the source is usually $6r_w$.

For 14.5 Ghz sources and B^+ ions, we get $B_m = 4.5 \ kGauss$ and $r_w > 218 \ cm$, while taking 28 Ghz and B^{++} ions we reduce down to $r_w > 57 \ cm$, still a very large size for ECR ion sources, but possible.

It should be observed that lower energy $100 keV/u$ B^+ beams , which require the same radius $r_w > 57 \ cm$ of the latter case, may be more favourable from the energetic point of view, depending on hydrogen heating. The cross section is indeed poor ($10^{-27}cm^{-2}$) as long as the hydrogen is cold, but it can be improved over the previous value of $0.5 \ 10^{-24}cm^{-2}$ if the hydrogen is heated up; for comparison the thermal equilibrium with this boron beam implies a $1 \ MeV$ temperature for the hydrogen. Detailed studies of plasma heating and rotation are then needed.

V) 3 POSSIBLE EXPERIMENTS AT LEGNARO

Almost all ECR ion sources support also an atomic physics program [41],[42]; some are specialized in it [6], [43] . The extraction voltage of the source $20kV$ is often enough for many experiments, but the use of the platform acceleration (up to 300 kV) projected for Alice adds the possibility to scan velocities up $\beta \cong 0.01 = 1.4\alpha$, that is the relevant medium beta regimes. The ATLAS linac has a similar platform installed [44] . We show that also the RFQ may be of use in order to send some ion beam back to the source with the desired energy.

We outline three experiments, in increasing order of complexity and interest, which can be considered for starting an atomic physics program in Legnaro. All atomic physics experiments may seem very simple, and indeed we propose here a minimal amount of additional hardware to what is paid for by the Alpi project.

Yet the need of background reduction may lead to additional costs: for example, the beam scattering from residual gas must be minimized, which implies longer transfer lines from the source analysis magnet walls, where outgassing happens, and requires eventually some ionic pumps near the measuring sets. In that respect, Alice has all metal seals and a strong pumping. Moreover, the UV or X-ray emitted by beam loss or beam impact or others can blind several detectors, so that suitable protections must be devised [45].

i) *Auger electron from a metal surface under high charge ions impact*

In Fig 4 , you can see a small metallic target enclosed in a biased section of the beam pipe. The $5 keV/u$ beam enters through slits and is decelerated down to $100 eV/u$. Varying the voltage V_{tp} between the target and a collector around the target, we can discriminate the collected electrons. Removing the collector we can also observe electron spectra at different angles.

Very roughly, we can expect that the metal behaves as a big neutral atom B in the transfer ionization model, with $I = k\Phi$ where Φ is the extraction work and k electrons are transferred. Since Φ is small (few eV) , we can expect that two or more electrons are transferred in the high n level of A , so that the resulting Auger emission is a simple determination of the energy levels of A . There are indications [46] that faster transfer ionization channels are possible for the metal ion system.

A related experiment [47] is the analysis of the sputtering of B induced by exciting the electrons of B with the potential energy of A^{z+} (usually the sputtering is due to the vibration of the crystal lattice hit by incident atom). In Fig. 4 scheme, a system for collimating, focusing and decelerating the beam is indeed included, for the sake of varying the incident kinetic energy.

The Auger electron emission of ions falling onto the ECR ion source walls was deemed to have an important effect on the ECR operation, because of the need to sustain the microwave discharge with fresh electrons. We note that Auger electrons and electrons supplied by ad hoc guns have kinetic energies of the same order ($300\ eV$).

ii) *A two beam experiment: how many sources?*

The very fact that ion-ion transfer ionization is possible with relevant cross sections (see Eq. (16)) motivate us to a research effort similar to what is usually developed for studying the ion atom collisions. While ions may exist also in a plasma, the need of controlling the experimental parameters implies the use of two beams, A^{z+} and B^{t+} .

This compares negatively with the ion-atom case at $E/A \cong 10 keV$, where the target was simply a noble gas in most cases, or molecular hydrogen. Experiments at very low energies $E/A \cong 10\ eV$ can not follow this simple scheme: since the ion beam must be propagated with $E/A \geq O(1 keV)$ to avoid defocusing and absorption in the target, the neutral atom B must be moving with A [45] . Managing a $10 keV/u$ neutral beam is notoriously difficult.

It is therefore apparent that a two ion beam merging facility, at the price of an initial complication, may scan a wide energy range: in Fig 5 , we envision a not symmetric facility, where a A^{z+} beam comes from the ECRIS platform (total accelerating voltage from 10 to 320 kV) while the beam B^{t+} comes from a lower energy beam line (an accelerating voltage 5 to 30 kV may be practical), here called the B-line.

The choice of "comoving" beams is preferred with respect to crossed beam due to the longer beam superposition (luminosity is an issue) and is preferred to colliding beam for the need of reaching lower collision energies. The two beams are merged by a dipole (in Fig. 5 we assumed that the magnetic rigidity of A is greater than the rigidity of B), they are propagated in a long merging section focused by Glaser or Einzel lens and are separated in a spectrograph magnet. The exit positions of A^{z+} and B^{t+} may be easily computed, enabling us to provide adequate dumps in order to minimize outgassing, background electrons and photon emission.

The dump of B involves only two boxes, the inner one biased up to $+29\,kV$, so that it can be easily moved inside the spectrograph vacuum chamber. The dump of A is a long tube, possibly with bends, since decelerating A is impractical.

In fig. 5 we show also the measuring positions for $A^{(z-1)+}$, $A^{(z-2)+}$ and so on . Experimental techniques include A and B beam chopping for increasing signal to noise ratio.

The most serious concern about the B-line is the need of an another source for it: in the important case of studying the A^{z+} collision against the same element A^{s+}, a second source is not strictly needed, but it simplifies beam handling. We can consider simpler sources (PIG, laser sources, a 2.45 Ghz ECRIS) as candidates for the B-line. Intensity is a need, and rules out recoil ion sources, Electron Beam Ion Sources, and so on.

Once a B-line source is installed, it is worthwhile to equip it with two analysis deflectors, with a gas cell in between [6,7], in order to produce and select metastable states.

iii) *Passing beams through Alice*

The standard Alice analysis dipole magnet [48] with a bending radius $R = 50\,cm$ guarantees a bending magnetic field $B_d = 4\,kGauss$ which permits to analyze B^{++} ions up to $64\,keV/u$. In Fig. 6 we envision the equipment needed to send a $64keV/u$ B^+ beam into Alice. We inject from the extraction region: we add a second standard analysis dipole in the head region, we put a removable plasma chamber which allows the B^{u+} beam to pass into Alice; we also add a second accelerating column to the Alice platform and a debuncher and a transfer line from the RFQ.

Note that Alice both produces the B^+ beam and is the transfer reaction plasma target: as a target, the beam fraction f may go from 0.002 to 0.2 , depending on estimates or measures from experiment ii).

Nominal platform voltage was held at 300 kV (it must be $> 170\,kV$ for B^+ injection into the RFQ). This beam should be focused in a 3 mm radius at the Alice extractor.

We provide a measuring position for neutral boron, if some is produced thanks to electron capture inside Alice. Particular care should be taken in the design of a proper beam dump for the B^+ ; in particular, we can assume that $c\sqrt{22M_pE}/eRB_d$ is held constant at 1/4 during the delicate measuring of the B^0 beams. Then the B^{z+} deflections for $z = 1, 2, 3, 4, 5$ are, respectively 11,28, 63, 90, 98 degrees; here we assumed a 20 cm effective pole width as in our standard magnet. The beam dump should then cover the range from 8 to 66 degrees.

Let alone its relevance to the section IV) concepts, this experiment may offer a first measurement of global ECR properties, such as the ionization rate.

VI) CONCLUSION

The installation of the ion source Alice, the RFQ and the ALPI linac will provide both the competence and the possibility to perform sophisticated atomic physics experiments at several energies, spanning from $E_{cm} = 10eV/u$ to $10^7 eV/u$. Direct relation of atomic physics to nuclear physics were outlined. Few basic experiments were envisioned, including ion-ion atomic collisions and beam-plasma interaction into Alice. A better understanding of the physics of ions is basilar for the high-Z element plasma physics and for advanced schemes of accelerator beam manipulation. A theory of beam trapping into ECRIS was introduced here.

APPENDIX A) TRAPPING KINEMATICS IN MIRROR LIKE GEOMETRY

With the nucleon number scaled quantities $\vec{P} \leftarrow \vec{P}/A$ and $q = ez/cA$, the scaled hamiltonian $h = 2m_p H/A$ is

$$h = \left(\frac{P_\vartheta + qA_\vartheta}{r}\right)^2 + (P_z + qA_z)^2 + P_r^2 \qquad (A.1)$$

where $A_z(r, \vartheta, z)$ represents the hexapole field and $A_\vartheta(r, z)$ represents the solenoid field. No electrostatic field can be held through a plasma (apart from sheaths at the border, few tens of Volt, and even smaller ambipolar potential inside).

Since the mirror distance is much larger than the ECRIS radius, it is useful to assume the following approximations in practical computation:

$$A_\vartheta = \tfrac{1}{2}B(z)r^2 \qquad\qquad A_z = \tfrac{1}{3}a(z)r^3 \sin(3\vartheta) \qquad (A.2)$$

where $a(z)$ and $B(z)$ are slowly changing. In particular $B(z)$ is the magnetic field $B_z(z)$ on the axis.

i) *The mirror case*

When no hexapole is included, h and P_ϑ are invariant of the motion, since the hamiltonian is cyclic in ϑ . Note that $h \geq 0$. Notwithstanding the fact we can not integrate the motion, still we can say exactly where the motion is not possible.

Let us indeed define the function

$$F_-(z; P_\vartheta) = \min_r \min_{p_r} \min_{p_z} h(r, z, p_r, p_z; P_\vartheta) \qquad ; (A.3)$$

evidently the fact a particular point is visited by the motion implies $F_-(z; P_\vartheta) \leq h$ (arguments after the semicolon will be dropped for brevity). Compare F_- with the Stormer potential (p. 49 in Ref. 12) .

We readily find

$$F_-(z) = \min_r \left(\frac{P_\vartheta + qA_\vartheta(r, z)}{r}\right)^2 \qquad (A.4)$$

When P_ϑ has the opposite sign of A_ϑ , $F_- = 0$ and motion is possible. In the not trivial case when they have the same sign, we compute F_- from (A.2) :

$$F_-(z) = 2qP_\vartheta B(z) \qquad (A.5)$$

With no collision only $B(z)$ can vary during the motion. In Fig. 7 curve a) you can see the situation corresponding to Fig. 3 , with the beam free to enter and exit from one side of the ECRIS .

When an atomic collision happens at a point (r', z') , we can assume that the velocity $\vec{v}$ of the beam is conserved. Its scaled charge q changes to q' and consequently the canonical momentum

$$P_\vartheta = p_\vartheta - qA_\vartheta$$

changes; since the mechanical momentum p_ϑ does not change during the atomic collision thanks to our assumption about $\vec{v}$, we find

$$P'_\vartheta = P_\vartheta - (q' - q)A_\vartheta(r', z') \qquad (A.6)$$

After the collision the motion continues to other points z'' with the new q' and P'_ϑ , so that F'_- is:

$$F'_-(z'') = F_-(z'') + 2(q' - q)\left(P_\vartheta - \tfrac{1}{2}q'r'^2 B(z')\right) B(z'') \qquad (A.7)$$

Let us discuss the increase of ionization $q' > q$ and the case $P_\vartheta > 0$, $B(z) > 0$; B_M be the lower of the two maxima of $B(z)$. From (A.7) if, and only if, the collision point satisfies

$$r'^2 < \frac{2P_\vartheta}{q'B(z')} \qquad (A.8)$$

the particle is promoted to an uniformly higher F_- curve (curve b in Fig 7) and may be trapped provided that we suitably choose the injection energy:

$$2qP_\vartheta < \frac{h}{B_M} < 2q'P_\vartheta - q'(q' - q)r'^2 B(z') \qquad (A.9)$$

(that is, we put only a little more energy than it was required to enter the mirror, so that when the mirror effect strengthens as an effect of the increased charge, the particle is trapped) .

The necessary and sufficient trapping condition (A.8) must be rewritten in order to see when it is satisfied. We can derive only a necessary condition from it now; indeed let us show that necessarily $r' > r_1$.

From (A.1) , referring to the period before the collision, we know that

$$h \geq \left(\frac{P_\vartheta + qA_\vartheta}{r}\right)^2$$

12

where the equality holds only at the very special instants when $p_r = 0$ and $p_z = 0$. From (A.2) solving the quadratic inequality we find

$$r \geq r_1(z) \equiv \frac{1}{qB(z)} \left(\sqrt{h} - \sqrt{h - F_-(z)} \right) \qquad (A.10)$$

which also holds at the collision point (r', z') ; comparing with (A.8) , we get

$$F_-(z') < \frac{h}{1 + (q' - q)^2 / 4qq'} \qquad (A.11)$$

This (not sufficient) condition is not difficult to satisfy: for the case $q' = 2e/cA$ and $q = e/cA$, we get $F_(z') < 8h/9$, limiting the trapping region to a slightly smaller segment than the mirror distance ; Eq. (A.11) is represented with a dashed line in Fig. 7).

ii) *The ECRIS case*

When the hexapole is included, the canonical angular momentum is no longer a motion invariant, so it is convenient to find an average canonical momentum I_ϑ and an effective hamiltonian h averaged from $\vartheta = 0$ to $\vartheta = 2\pi/3$ which is the period of the hexapole. Then collisions alter the value of q and I_ϑ , but not that of h, in a way dependent on the actual collision position (as above, less than half of the collisions lead to trapping). Here we will obtain I_ϑ as a function of h and slowly changing variables.

In performing an average on the fast varying components, we note that $B(z)$ and $a(z)$ are slowly changing functions of z, and so will P_z change from its hamiltonian equation of motion (z may have fast oscillations, but they cause negligible changes of $a(z)$).

Since h depends substantially from r we can not ignore r and p_r oscillation; moreover they are forced exactly with the periodicity 3ϑ . So we decompose

$$r = \bar{r} + \tilde{r} \qquad P_r = \bar{P}_r + \tilde{P}_r \qquad (A.12)$$

where $\tilde{r}$ contains $\exp(-3i\vartheta)$ and harmonics, while $\bar{r}$ self-consistently varies with a frequency slower — and what is most important — not resonant with $3d\vartheta/dt$.

Under these conditions:

$$I_\vartheta(\bar{r}, \bar{P}_r; z, P_z, h) = \frac{3}{2\pi} \int_0^{2\pi/3} d\vartheta \, P_\vartheta(\vartheta, \bar{r} + \tilde{r}, \bar{P}_r + \tilde{P}_r; z, P_z, h) \qquad (A.13)$$

is an adiabatic invariant of the motion.

Explicitly P_ϑ is

$$P_\vartheta(\vartheta, \bar{r} + \tilde{r}, \bar{P}_r + \tilde{P}_r; z, P_z, h) = -\tfrac{1}{2}qB(z)r^2 + r\sqrt{h - P_r^2 - (P_z + \tfrac{1}{3}qa(z)r^3 \sin 3\vartheta)^2} \qquad (A.14)$$

and may play the role of a hamiltonian with respect to the flowing of 3ϑ :

$$\frac{dr}{d\vartheta} = -\frac{\partial P_\vartheta}{\partial P_r} \qquad \frac{dP_r}{d\vartheta} = -\frac{\partial P_\vartheta}{\partial r} \qquad (A.15)$$

13

Let us assume that $a\bar{r}^2/B$ is a small parameter, and we want to keep up to the first correction a^2 in the final result. Then $\tilde{r}$ and $\tilde{p}_r$ are of order of a , so that we can linearize Eq. (A.15) around $\bar{r}$ and solve it. With the notation $\Gamma = (h - \bar{P}^2 - P_z^2)^{-1/2}$, we get

$$\tilde{r} = \Re \frac{\Gamma^2 \bar{r} D_3}{\Gamma \bar{r}(qB(z) + (7/6)\Gamma q^2 a^2 \bar{r}^5) - 9 - 3i\Gamma \bar{P}_r} \qquad D_3 = \frac{8}{3} P_z q a \bar{r}^3 i \exp[3i\vartheta] \quad (A.16)$$

where the driving force D_3 is apparent; there is another force driving the oscillation of $\tilde{r}$, but it is formally smaller: $D_6 = (7/36)q^2 a^2 \bar{r}^6 \exp[6i\vartheta]$.

Expanding Eq. (A.13) in powers of $\tilde{r}$, and using Eq. (A.15) , we find

$$2\pi I_\vartheta = \oint d\vartheta \left(P_\vartheta(\vartheta, \bar{r}, \bar{P}_r) - 2\tilde{p}_r \frac{\partial \tilde{r}}{\partial \vartheta} \right) = \oint d\vartheta \left(P_\vartheta(\vartheta, \bar{r}, \bar{P}_r) - \frac{2}{\bar{r}\Gamma} \left(\frac{\partial \tilde{r}}{\partial \vartheta} \right)^2 \right) \qquad (A.17)$$

Substituting Eqs. (A.14) and (A.16) as it is required by Eq. (A.17) , we find finally

$$I_\vartheta = -\tfrac{1}{2} qB(z)\bar{r}^2 + \bar{r}\sqrt{h - \bar{P}_r^2 - P_z^2} +$$

$$-q^2 a^2 \Gamma^3 \bar{r}^7 \left(\frac{h - \bar{P}_r^2}{36} + 32 \frac{P_z^2}{(\Gamma \bar{r}(qB(z) + (7/6)\Gamma q^2 a^2 \bar{r}^5) - 9)^2 + 9\Gamma^2 \bar{P}_r^2} \right) \qquad (A.18)$$

The first two terms give exactly the unperturbed hamiltonian. The hexapole first averaged correction a^2 turns up in the form of an effective contribution to A_ϑ ; in particular this gives an effective contribution to B_z which vanishes as $\bar{r}^5$ near the source axis, and contributes to the focusing: this is expected since the hexapole is seen from the rotating ion with alternating signs, giving therefore a strong focusing. A notable coupling with P_z emerges.

Since the new contribution goes as $\bar{r}^5$, we do not expect new qualitative effects in the overall beam circulation, but only a complicate explicit form of the trapping potential $F_-(z, I_\vartheta)$. Quantitative analysis of the trapping conditions is in progress.

REFERENCES

[1] P.J. Mohr , *Nucl. Instr. Meth.* **B31**, 1, (1988) and following papers.

[2] A. Barany , H. Danared, *Nucl. Instr. Meth* **B23**, 1 (1987)

[3] P.J. Mohr *At. Data Nucl. Data Tables*, **29** 453 (1990)

[4] R.D. Deslattes, *Nucl. Instr. Meth* **B24/25**, 52 (1987)

[5] R.Geller, *Jour. de Phys.*, **50**, C1-887 (1989)

[6] M. Delaunay, S. Dousson, R. Geller, B. Jacquot, D. Hitz, P. Ludwig, P.Sortais, S. Bliman, *Nucl. Instr. Meth.* , **B23**,177 (1987)

[7] M. Druetta, T.Bouchama, S. Martin, *Nucl. Instr. Meth.* , **B40/41**, 50 (1989)

[8] N.J. Peacock , H.P. Summers, *Nucl. Instr. Meth* **B23**, 226 (1987)

[9] C.J. Liu, N.B. Mansour, Y.Azuma, H.G. Berry, D.A. Church, R.W. Dunford, *Phys. Rev. Lett.*, **64**, 1354 (1990)

[10] J.Arianer, *Nucl. Instr. Meth.* **B9**, 516 (1985)

[11] G.Melin, F.Bourg, P.Briand, J.Debenardi, M.Delaunay, R.Geller, B. Jacquot, P.Ludwig, T.K. N'Guyen, M. Pontonnier, P.Sortais, *Jour. de Phys.*, **50**, C1-673

[12] K.Miyamoto *Plasma physics for nuclear fusion*, The MIT Press, Cambridge, (1987).

[13] R.K. Janev , *Jour. de Phys.*, **50**, C1-421 (1989)

[14] " Proceedings of the Int. Symposium on heavy ion inertial fusion" (ed D.Judd, to appear as a special issue of *Particle Accelerators*), held at Monterey (CA), December 3-6 1990.

[15] B. Langdon "Chamber propagation" in Ref 14

[16] C.Rubbia , *Nucl. Instr. Meth.* , **A278**, 253 (1989)

[17] I. Hofmann "Advanced driver concept and relevant machine experiments", in Ref. 14

[18] R. W. Muller "Examples of heavy-ion ICF driver schemes for indirect drive" in Ref. 14

[19] K.Kilian "Cooling by inelastic intrabeam scattering of partially ionized ions" in *Proceedings of the Workshop on Electron Cooling and new Cooling Technoques* (ed. L.Tecchio, R.Calabrese, World Scientific, Singapore, 1991) held at Legnaro, May 15-17 1990.

[20] J.Eichler *Phys. Reports*, **193**, 165(1990)

[21] B. Muller "QED of strong fields" pg. 41 in *Quantum Electrodynamics of strong fields* (ed. W.Greiner, Plenum, New York, 1983)

[22] F.Bosch "Experiment on the excitation of the innermost electrons in extremely strong fields" pg. 155 in Ref. 21

[23] E.Teller, *Nucl. Instr. Meth.*, **B24/25**,1 (1987)

[24] A.V. Timofeev "Cyclotron Oscillations of an Equilibrium Plasma" pg 63-252 in *Reviews of Plasma Physics*, **14**, Plenum, New York, (1989)

[25] M.Cavenago, G. Bisoffi, "Optimization studies of a 14.4 GHz ECR ion source for the superconductive linac at Legnaro", *Nucl. Instr. Meth. A*, **A301**, 9 (1991)

[26] *Proceedings of the 10th Int. Workshop on ECR ion sources* (ed F.Meyer, M.I.Kirkpatrick, Oak Rigde National Laboratory, CONF-9011136, 1991) held at Knoxville, November 1-2 1990.

[27] R.Geller, private communication.

[28] P.Beiersdorfer, A.L. Osterfeld, M.H. Chen, J.R. Henderson, D.A.Knapp, M.A. Levine, R.E. Marrs, K.J.Reed, M.B.Scheidner, D.A. Vogel, *Phys. Rev. Lett.*, **65**, 1995 (199

[29] J.R. Henderson, P.Beiersdorfer, C.L.Bennet, S. Chantrenne, D.A.Knapp, R.E. Marrs, M.B.Scheidner, K.L Wong, G.A. Doschek, J.F. Seely, G.A. Brown, R.E. LaVilla, J. Dubau, M.A. Levine, *Phys. Rev. Lett.*, **65**, 705 (1990)

[30] H.I. West "Calculation of ion charge-state distribution in ECR ion sources", Report UCRL-53391, University of California, Lawrence Livermore National Laboratory.

[31] T.A. Antaya, *Jour. de Phys.* , **50**, C1-707 (1989)

[32] H.B. Gilbody, *Nucl. Instr. Meth* **B23**, 30 (1987)

[33] H. Ryufuku, K. Sasaki, T. Watanabe, *Phys. Rev.* **A 21**, 745 (1980)

[34] A.Salop, R.E. Olson *Phys. Rev.*, **A13**, 1312 (1976)

[35] A.Barany, G.Astner, H.Cederquist, H.Danared, S. Huldt, P. Hvelplund, A.Johnson, H.Knudsen, L.Liljeby, K.G. Rensfelt, *Nucl. Instr. Meth.* **B9**, 397, (1985)

[36] A. Niehaus, *Nucl. Instr. Meth* **B31**, 359 (1988)

[37] N.Rostoker, H.U. Rahman *Comments Plasma Phys. Controlled Fusion*, **10**, 81 (1986)

[38] J.G.Linhart, *Plasma Phys. Control Fusion*, **30**, 1641 (1988)

[39] B.C.Maglich, *Nucl. Instr. Meth*, **A271**, 13 (1988)

[40] R. Feldbacher, M. Heindler, *Nucl. Instr. Meth.* , **A271**, 55 (1988)

[41] D.J. Clark, C.M. Lyneis, M.H.Prior, R.G. Stokstad, S.Chantrenne, P.O. Ogan, *Nucl. Instr. Meth.*, **B40/41**, 6, (1989)

[42] O.Vogel *Physica Scripta*, **42**, 341, (1990)

[43] F.W. Meyer, J.W. Hale, *Rev. Sci. Instr.*, **61**, 324 (1990)

[44] R.W. Dunford, H.G. Berry, C.J. Liu, M. Hass, R.C. Pardo, M.L.A. Raphaelian, B.J Zabransky, *Nucl. Instr. Meth.* , **B40/41**, 9, (1989)

[45] C.C. Havener, M. S. Huq, H.F.Krause, P.A. Schulz, R.A. Phaneuf , *Phys. Rev.* , **A39**, 1725 (1989)

[46] P.A. Zeijlmans van Emmichoven, C.C. Havener, F.W. Meyer, "The neutralization of highly charged ions grazingly incident on a metal surface", to appear in *Phys. Rev A*.

[47] D.L Weathers, T.A. Tombrello, M.H. Prior, R.G. Stokstad, R.E. Tribble, *Nucl. Instr. Meth.* , **42**, 307, (1989)

[48] M.F. Moisio, private communication.

TABLE I *(Partial) overview of atomic physics source and topics*

Energy & type / Source	Ion on atom	Ion on ion	Fast ion on atom or ion	One, two e⁻ ions
Beam foil	no	no	yes, with noise	yes, with noise
ECR	yes, high current	yes	yes, high current	only low $Z < 20$.
EBIS	yes, limited current	yes, limited current	yes, limited current	yes
Recoil sources	yes, low current	no	no	only low $Z < 20$ with noise

Source / Physics output	Ion on atom	Ion on ion	Fast ion on atom or ion	One, two e⁻ ions
Physics output	Plasma theory (ECR, tokamak, EBIS), atomic structure, X-ray lasers.	Plasma theory (ECR, tokamak, EBIS, trapping), atomic structure	Atomic structure ICF.	**Q.E.D.**

FIGURE CAPTIONS

1) *A horizontal section of the source body.* The iron yoke, the two coils and the hexapole are symmetric around the z-axis. The first stage is located inside the small iron ring. The backbone plane is partly visible. Two out of 12 coil contacts are shown.

2) *A vertical section of the source head.* All the feedthroughs are mounted on the head of the source. Observe the waveguide path and the second stage cavity RF mesh.

3) *Injecting boron into a Very Large ECR ion source* The roughly helical path (solid line) of the injecting beam B^+ is shown, omitting the larger part of the return travel for clarity. Two collision events are shown, each originating a B^{++} trajectory (heavy solid lines).

4) *Scheme of an Auger electron apparatus* The Alice beam is focused onto a rotable target, and options (removable collector, spectrometer arm) are provided with the purpose of analyzing the emitted particles. The dashed electrical connection are optional.

5) *A multipurpose beam-beam facility* The A beam from the Alice platform is merged with another beam from an auxiliary line, equipped with a gas cell and two analysis magnets, and the rection products are then separated in a larger magnet. Note the beam dumps.

6) *Passing a charged beam into Alice* The B^+ beam (heavy solid line), coming back from the RFQ at the designed angle of 10^0 with Alice axis, is steered and bent in order to match the Alice extractor hole; charged interaction products (a solid line) are measured by the Faraday cup and a port is available for neutrals (heavy dashed line).

7) *The trapping conditions* Ion motion is possible only when $F(z)$ (heavy solid line) is below h (solid line). A collision (transition) changing the F curve from a) to b) is shown, resulting in the ion trapping. Trapping may happen only when curve a) is below the dashed level.
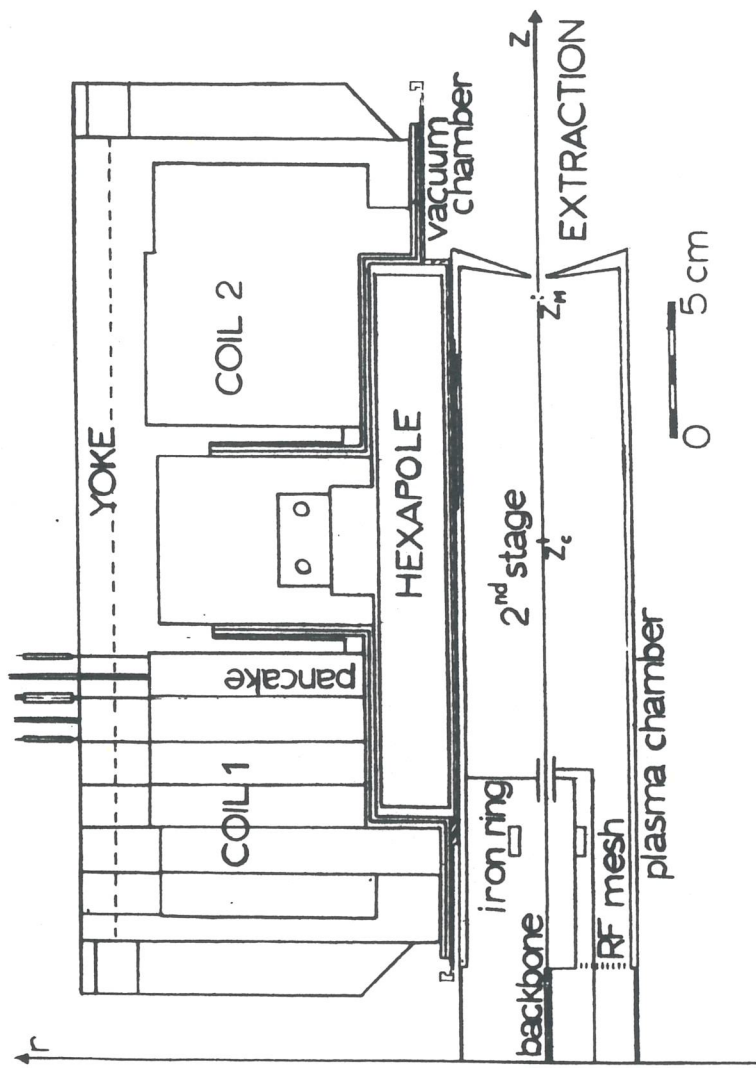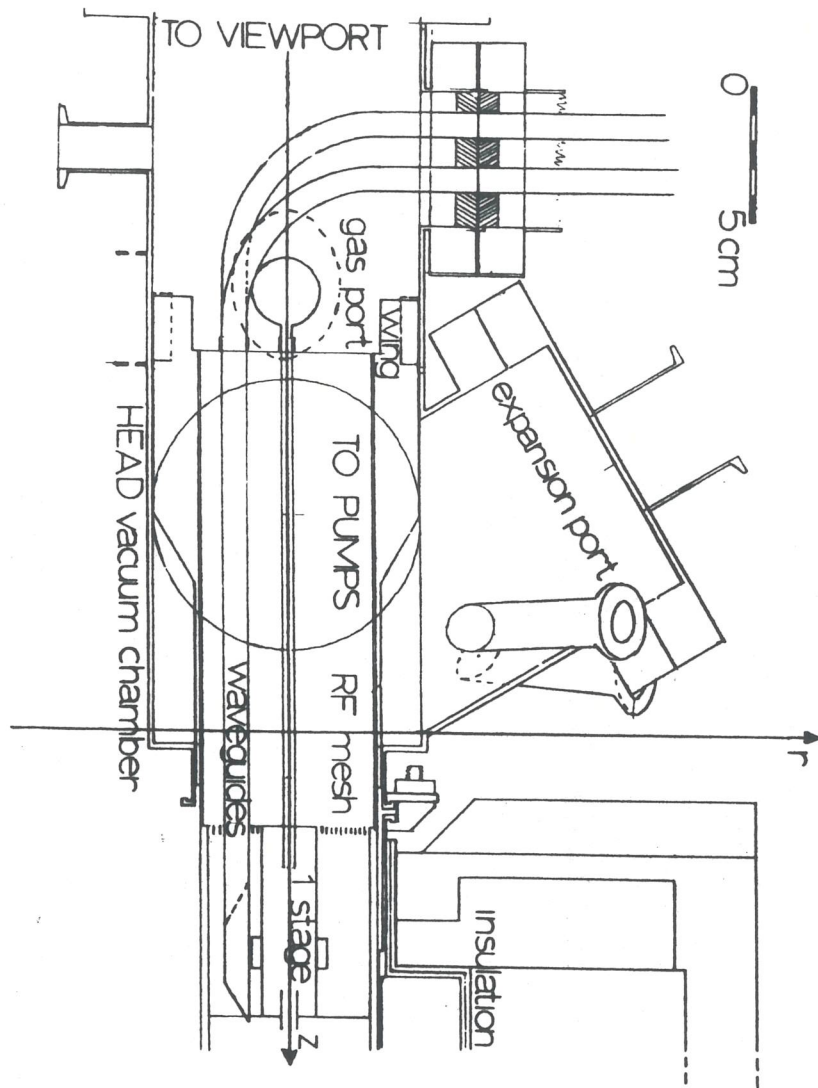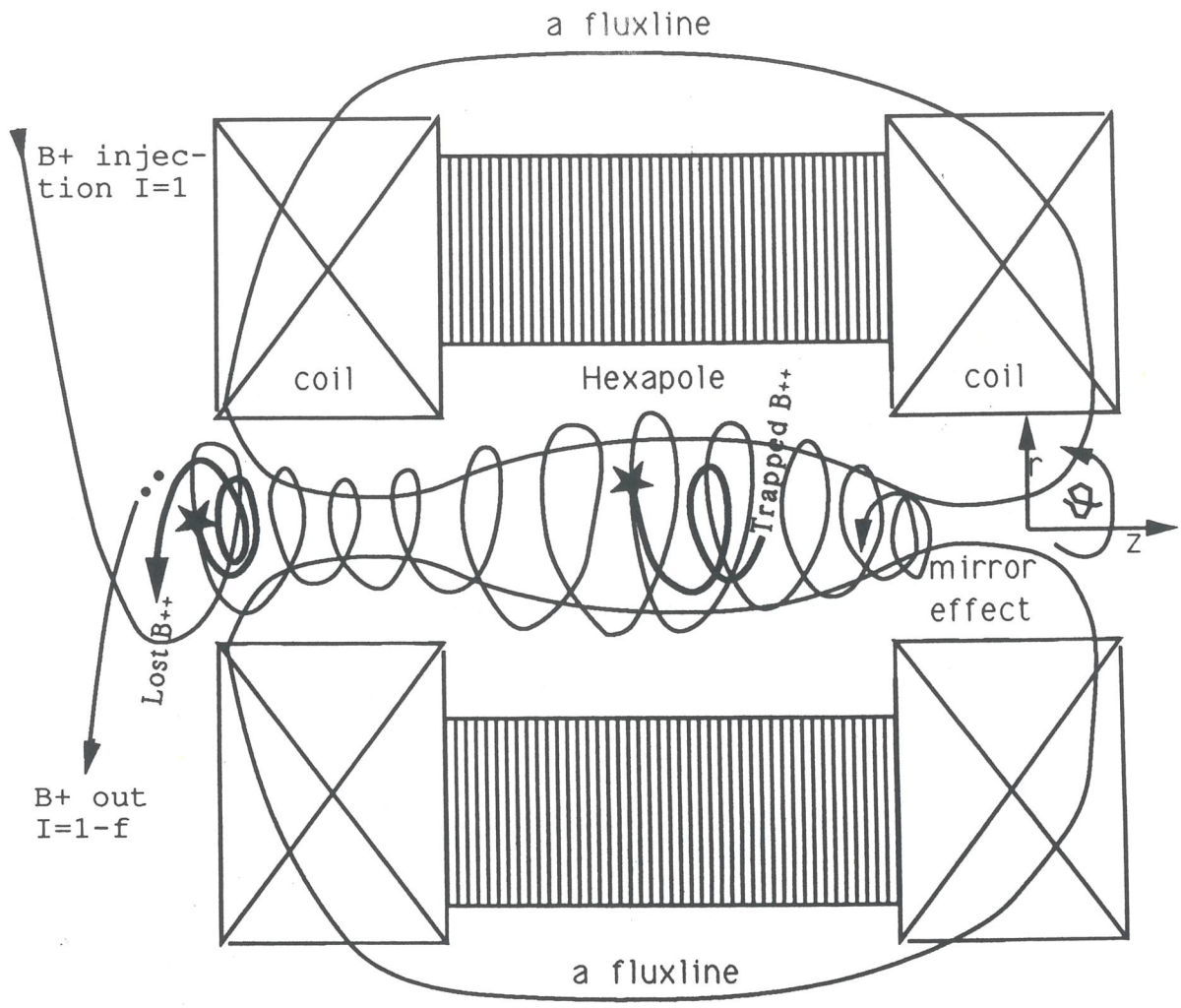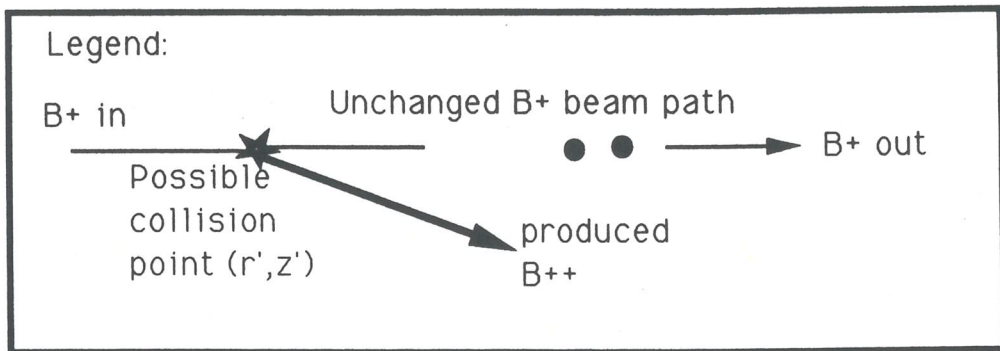
Fig 1

19

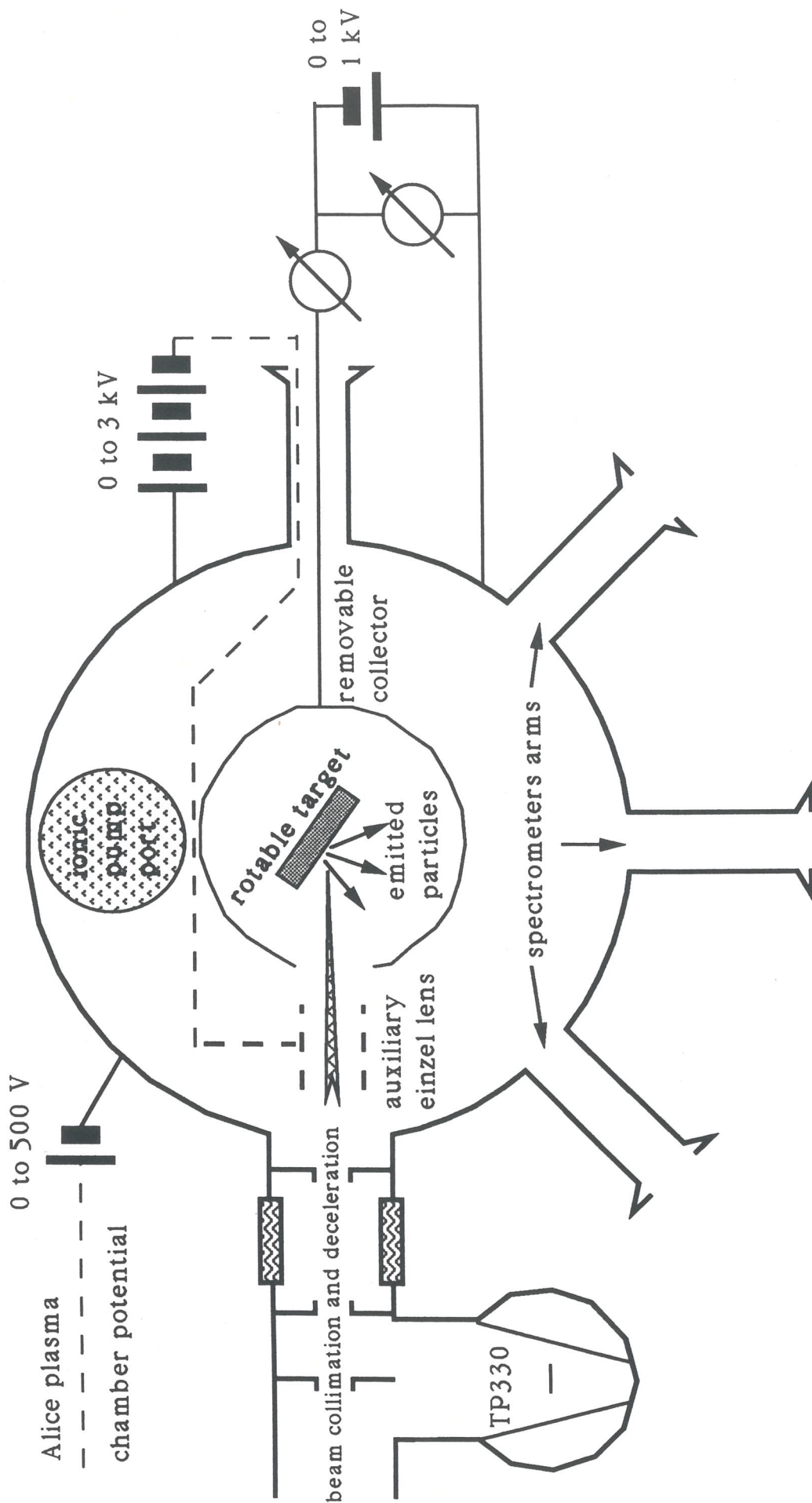Fig 2)

Fig **3**) Injecting boron into a Very Large ECR ion source

Fig 4) Scheme of an Auger electron detection apparatus

0 to 1 kV

0 to 3 kV

ionic pump port

rotable target

removable collector

emitted particles

auxiliary einzel lens

spectrometers arms

0 to 500 V

Alice plasma

chamber potential

beam collimation and deceleration

TP330

Alice

Platform

300 kV column

Beam A

B-line

Blice
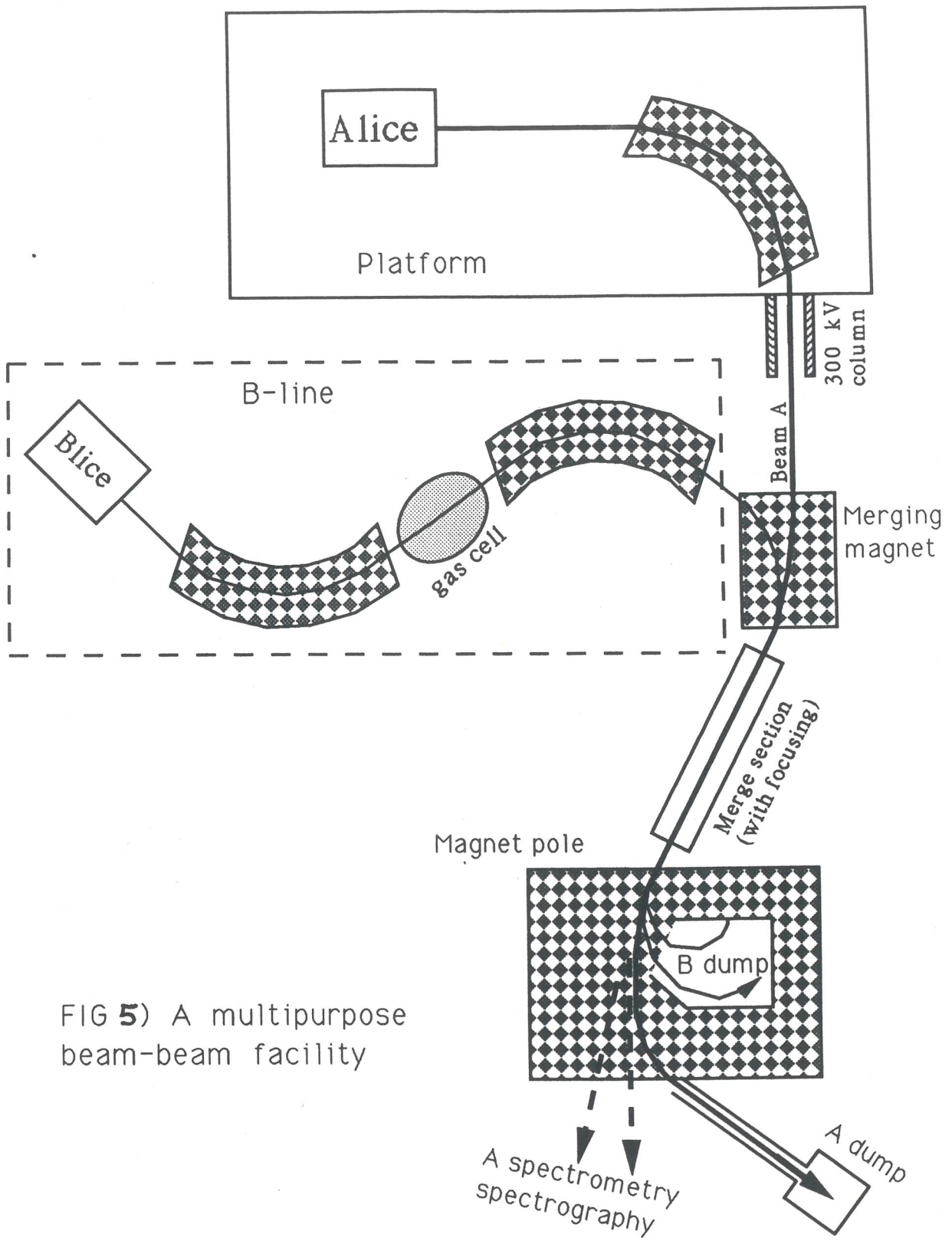
gas cell

Merging magnet

Merge section (with focusing)

Magnet pole

B dump

FIG 5) A multipurpose beam-beam facility

A spectrometry spectrography

A dump